Treatment of VLCAD deficient patient fibroblasts with peroxisome-proliferator activated receptor δ agonist improves cellular bioenergetics

Olivia D'Annibale
University of Pittsburgh
Yu Leng Phua
University of Pittsburgh
Clinton Van't Land
University of Pittsburgh
Anuradha Karunanidhi
University of Pittsburgh
Alejandro Dorenbaum
Reneo Pharmaceuticals, Inc.
Al-Walid Mohsen
University of Pittsburgh
Jerry Vockley (vockleyg@upmc.edu)
University of Pittsburgh

Article

Keywords: fatty acid oxidation, VLCAD deficiency, ACADs, PPARs, acyl-CoA dehydrogenases, REN001, cellular bioenergetics

Posted Date: April 20th, 2022

DOI: https://doi.org/10.21203/rs.3.rs-1530711/v1

Abstract

Very long chain acyl-CoA dehydrogenase deficiency (VLCADD) is an autosomal recessive disease that prevents the body from utilizing long chain fatty acids for energy, most needed during stress and fasting. Symptoms can appear from infancy through childhood and adolescence or early adulthood, and include hypoglycemia, recurrent rhabdomyolysis, myopathy, hepatopathy, and cardiomyopathy. REN001 is a peroxisome proliferator activated receptor delta (PPARδ) agonist that modulates gene expression of fatty acid β-oxidation enzymes and oxidative phosphorylation proteins. VLCADD fibroblasts responded differently to REN001 based on genotype. All cells had statistically significant increases in *ACADVL* gene expression. Small increases in VLCAD protein and enzyme activity were observed and were cell line and dose dependent. Cellular bioenergetics improved in all REN001 treated fibroblasts as demonstrated by oxygen consumption rate and ATP production. VLCADD fibroblasts containing missense mutations responded better to REN001 treatment than one containing a duplication mutation in *ACADVL*. REN001 treated VLCADD fibroblasts results in an increase in VLCAD protein, enzyme activity, and a decrease in cellular stress. These results establish REN001 as a potential therapy for VLCADD as enhanced expression may provide therapeutic increase in total VLCAD activity but suggests the need to mutation specific treatment augmented by other treatment measures.

Introduction

Long chain fatty acids enter cells *via* protein fatty acid transporters on the cell surface concurrent with or followed by conjugation to a CoA group by a fatty acyl-CoA synthase (FACS) [1, 2]. Long chain fats are activated in the cytoplasm and require a series of three enzymatic steps that constitute what is known as the carnitine cycle [1, 2]. Carnitine palmitoyl transferase 1 (CPT1) replaces the CoA moiety of the long-chain acyl-CoA with carnitine (acylcarnitine), which is transported by carnitine-acylcarnitine translocase (CAT) across the inner mitochondrial membrane in exchange for a free carnitine molecule from the mitochondrial matrix [1, 2]. The carnitine of the acylcarnitine is replaced with a CoA and is released as an acyl-CoA ester by carnitine palmitoyl transferase 2 (CPT2), where it can then enter the fatty acid β-oxidation pathway, a series of four enzymatic steps that results in the production of a two carbon acetyl-CoA, one NADH, and one $FADH_2$, regenerating an acyl-CoA that is now two carbons shorter [1–3]. Very long-chain acyl-CoA dehydrogenase (VLCAD) catalyzes the a,b-dehydrogenation of long chain acyl-CoA substrates with various carbon chain length and maximal activity to C14-CoA, to its enoyl-CoA product utilizing the electron transfer flavoprotein (ETF), a mitochondrial matrix electron shuttle protein, as an electron acceptor [1, 2, 4]. Reduced ETF transfers its' reducing equivalents to its redox partner, the ETF dehydrogenase (ETFDH), which in turn delivers the reducing equivalents to the ubiquinone pool and complex III of the electrons transport chain (ETC) [1, 2, 4].

VLCAD deficiency (VLCADD) is an autosomal recessive disorder caused by biallelic mutations in *ACADVL* gene [5]. The frequency of VLCADD in various populations is about 1:30,000 to 1:100,000 live births [6, 7]. Symptoms of VLCADD include hypoglycemia, recurrent rhabdomyolysis, myopathy, hepatopathy, and cardiomyopathy. Symptoms can present in infancy, later in childhood, or in adolescence or early

adulthood [8]. Treatment for VLCADD patients involves a low-fat diet consisting mainly of medium chain triglyceride (MCT) or triheptanoin supplementation with smaller more frequent meals [9–12]. However, many patients still have episodes of rhabdomyolysis and cardiomyopathy that can lead to hospitalization suggesting the need for additional treatment options. Episodes of metabolic decompensation are typically triggered by physiologic stress such as illness or excess exercise, but the cause often remains unidentified [13]. Ultimate outcome is improved by identification of the disorder through newborn screening [14].

Peroxisome proliferator-activated receptors (PPAR) are nuclear receptors that play key roles in the regulation of fatty acid β-oxidation, lipid metabolism, inflammation, and cellular growth and differentiation [15–19]. They are divided into several categories based on the specific promotors that they stimulate. PPARδ is a major activator of oxidative metabolism and is ubiquitously expressed [15, 20, 21]. It is activated by polyunsaturated fatty acids such as arachidonic acid, oleic acid, dexamethasone, and eicosanoids such as prostaglandin 1 (PGA_1), carbaprostacyclin (cPGI), and 15-deoxy-$\Delta^{12,14}$-prostaglandin J_2 (15d-J_2) [22, 23]. *In vivo* experiments with PPARδ agonists have examined their effects in a variety of diseases and cellular processes including diabetes, obesity, and lipid metabolism. In a two week clinical study, treatment of moderately obese men with dyslipidemia with GW501516, a PPARδ agonist, resulted in a decrease in fasting and postprandial plasma triglycerides, low-density lipoprotein (LDL) cholesterol, apoB compared to placebo, as well as reduction in liver fat content and urinary isoprostanes (a marker of whole-body oxidative stress) [24]. Four weeks of treatment of insulin-resistant middle-aged obese rhesus monkeys with GW501516 induced a dose-dependent rise in serum high density lipoprotein cholesterol while lowering the levels of small-dense LDL, fasting triglycerides, and fasting insulin [25]. Genetically obese *ob/ob* mice had reduced plasma glucose and blood insulin levels after treatment GW501516 [20]. Genetically predisposed obese $Lepr^{db/db}$mice treated with GW501516 demonstrated a decrease in lipid accumulation, while PPARδ-deficient mice were prone to obesity on a high-fat diet [19]. Recent studies with herbal supplements such as bavachinin (a pan-PPAR agonist) from the glucose-lowering malaytea scurfpea herb and ginger (a PPARδ agonist) reduced obesity in obese *db/db* mice, and diet induced obesity in C57BL6J mice, respectively [26, 27].

REN001 (formerly known as HPP593), a PPARδ agonist (Reneo Pharmaceuticals), has been shown to reduce oxidative stress and inflammation in renovascular hypertensive Goldbatt's 2 kidney 1 clip (2KIC) rats [28]. 2KIC mice treated with this REN001 for 30 days had no necrosis in kidneys, reduced oxidative stress-responsive proteins, and decreased pro-death protein BNIP3 in kidney tubules [28]. REN001's proposed mechanism is the inhibition of BNIP3 activation resulting in preserved mitochondrial function and oxidative stress control.

Bezafibrate is a pan-PPAR agonist used to treat hyperlipidemia as it increases high density (HDL) cholesterol levels, decreasing total and LDL cholesterol levels [29]. Since PPARs can increase fatty acid β-oxidation there has been interest in repurposing bezafibrate as a treatment for fatty acid oxidation disorders. In an *in vitro* study, VLCADD patient derived fibroblast cell lines treated with two versions of bezafibrate demonstrated a 3-fold increase in palmitate oxidation with an increase in VLCAD mRNA,

protein, and enzyme activity. RT-PCR showed an increase in other genes encoding proteins in the β-oxidation pathway [30]. Similarly, treatment of CPT2 deficient human myoblast cells with bezafibrate, and the PPARα agonist GWδ 0742 led to an increase in *CPT1-B* and *CPT2* mRNA levels with increased CPT2 activity, while GWα 7647, another PPARα agonist, had minimal effect [31]. Treatment with bezafibrate of fibroblasts from 26 patients with mitochondrial fatty acid oxidation trifunctional protein (MTP) deficiency with various mutations led to improved cellular palmitate oxidation in 6 of 26 cell lines [32]. In an open label trial treating patients with CPT2 deficiency, patients showed an increased or no change in incidence of rhabdomyolysis episodes, but an improvement in quality of life scores [33, 34]. However, in a randomized double blind placebo control clinical trial in patients with VLCAD or CPT2 deficiency, bezafibrate failed to improve cardiac function or whole-body fatty acid oxidation [35]. One possibility for this dichotomy is the limited PPARδ effect of bezafibrate.

Finally, in a clinical study examining the effect of resveratrol, a mitochondrial antioxidant, had no effect on exercise tolerance or whole body fatty acid oxidation in patients with VLCAD or CPT2 deficiency. Thus, a clinical need for additional therapies for this group of disorders remains.

In this study, we examined the effects of REN001 in VLCADD patient derived fibroblast cell lines in advance of clinical trials with this agent.

Results

PPARδ agonists upregulates genes associated with fatty acid oxidation and mitochondrial ETC complexes

PPARδ agonists are known to upregulate transcription of FAO and ETC genes [15–21]. Despite the well-established association between PPARδ and improved FAO *in vitro*, the direct target genes of PPARδ remain unclear [36]. To deduce the binding profile and target gene repertoire of PPARδ in an unbiased and genome-wide manner, we re-assessed a prior PPARδ ChIP-seq data that was generated using HUVEC cells (GSE 50144) (PMID: 24721177) (Supplementary Fig. 1). MACS2 analysis of the ChIP-seq data identified a high enrichment of binding events (83%) that were localized to the intergenic region, with a consensus binding motif of GGTCAAAGGTCA that corresponds to PPARd under the family and class of thyroid hormone receptor-related factors (NR1): Nuclear receptors with C4 zinc fingers (JASPAR) (Supplementary Fig. 1A). Given the enrichment of PPARδ binding sites being primarily localized within 5 kb downstream of transcription start sites, such observation supports PPARδ primary role as a DNA enhancer (Supplementary Fig. 1B). Of note, functional interpretation of *cis*-regulatory regions of PPARδ binding peaks using GREAT and Cistrome GO analysis tools consistently revealed a high degree of confidence in the fatty acid metabolism pathway that is predicted to be enriched by PPARδ target genes (Supplementary Fig. 1C). Notably, PPARδ target genes were also found to be implicated in multiple human phenotypes that are highly reminiscent of FAO disorders, including, but not limited to, hypoglycemia, hepatic steatosis and rhabdomyolysis (Supplementary Fig. 1D).

To determine if REN001 increases transcripts associated with FAO, we quantified mRNA levels via real-time qPCR. In this manner, all control and VLCAD cell lines demonstrated statistical improvement in both FAO and ETC complexes at the transcript level (Fig. 1A-F). Specifically, all treated VLCAD cell lines demonstrated a statistically significant upregulation of *ACADVL* in response to either 30 or 120 nM REN001, with the VLCAD-1 cell line demonstrating at least 2-fold increase in *ACADVL* when treated with 120 nM REN001 (Fig. 1A). Similarly, *HADHA* and *HADHB*, the genes encoding for TFP subunits, also trended upwards with a small but statistically increase of transcripts (Fig. 1B, C). Consistent with the positive effects of REN001 on FAO-associated genes, we also observed upregulation of *ETFDH*. To deduce the overall specificity of REN001 and demonstrate that the gene expression changes are not attributable to an off-target effect, we analyzed *UQCRC2* (Complex III) and *NDUFS2* (Complex I), genes that are not known to be targeted by PPARδ agonists based on the ChIP-seq analysis (PMID: 24721177) (Supplementary Fig. 1E). Indeed, qPCR analysis showed minimal changes in both *UQCRC2* and *NDUFS2*, validating the veracity of drug target specificity for REN001 in our assay (Fig. 1E, F, Supplementary Fig. 1E). We decided to use Control-1 cell line for all subsequent experiments as all three control cell lines had a similar increase in mRNA, with Control-1 having the largest increase in *ACADVL* (Fig. 1A).

Induction of fatty acid oxidation proteins

VLCAD deficient patient derived fibroblast cell lines showed decreased VLCAD protein and/or enzyme activity that varied with the *ACADVL* mutation (Supplementary Fig. 2A; Supplementary Fig. 3A). Treatment with REN001 for 48 hr increased VLCAD protein only in cell line 3, with 2.1-fold increase when treated with 30 nM as demonstrated via western blotting (Fig. 2A). Neither of the other patient cell lines nor control cells showed significant changes in VLCAD protein signal, confirming the instability of mutant protein translated from the upregulate mRNA. Since PPARδ upregulates all the fatty acid β-oxidation genes, the level of TFPa and b subunits, the products of the *HADHA* and *HADAB* genes, respectively, was analyzed in patient cells. TFP is a component of the FAO/ETC macromolecular complex and interacts closely with VLCAD [4]. All cell lines had an increase in TFPa as demonstrated by western blotting (Fig. 2B). Control cells, along with patient cell lines 1 and 2 had increased TFPβ subunit across various concentrations (Figs. 2B, 2C). VLCAD-1 had a 1.7-fold change in TFPβ subunit at various concentrations of REN001, while patient cell lines 2 and 4 did not (Fig. 2C). Immunofluorescence (IF) staining of control fibroblast, FB826, was performed for VLCAD and HADHA antigens (Supplementary Fig. S3A). A 1.3-fold change in VLCAD was found with 30 nM REN001 via immunostaining (Supplementary Fig. S3B). Minimal change occurred in HADHA immunostaining both consistent with western blotting.

VLCAD enzyme activity

VLCAD enzyme activity was measured in patient and control cells treated with REN001. Not surprising, untreated VLCAD deficient patient derived fibroblasts had significant reductions in VLCAD activity while maintaining normal levels of medium chain acyl-CoA dehydrogenase (MCAD) activity measured as a control (Supplementary Fig. 4A). VLCAD deficient cell lines had a variable response to REN001. VLCAD-1 and – 3 had statistically significant increases in VLCAD activity at 60 and 120 nM concentrations, respectively. Neither VLCAD-2 nor VLCAD-4 showed increased activity. The control cell line showed a trend

of increasing VLCAD enzyme activity with increasing REN001 concentration that was not statistically significant. MCAD activity for all cell lines at most drug concentrations was unchanged, though VLCAD-3 treated with 60 nM REN001 was slightly decreased (Supplementary Fig. 4B). MCAD activity was not measured for VLCAD-4 due to a limited sample amount.

FAO Flux Assay

A whole cell [^{3}H]-oleate oxidation assay was used to measure overall flux through the fatty acid oxidation pathway and is a measure of VLCADD severity [37]. VLCAD-2, -3, and the control cell line no significant changes in oleate oxidation following drug treatment (Fig. 3). There was a trend towards an increase in flux in VLCAD-1 and VLCAD-4 suggesting minor improvement, but the change reached statistical significance only in VLCAD-4 treated with the highest concentration of REN001 (120 nM, Fig. 3). A minimal or no change in activity was not surprising as the mRNA and protein had small changes.

Whole Cell Oximetry

We have previously shown that VLCADD cells show impaired oxidative phosphorylation as measured by whole cell oximetry [38], including VLCAD-1 and − 2 used in this study. Oxygen consumption rate (OCR) was measured via a Seahorse XFe96 Extracellular Analyzer. The basal respiration was increased compared to control in all VLCAD deficient cell lines with an increase in maximum respiration and no change in spare capacity or ATP production, a pattern consistent with impaired oxidative phosphorylation and mitochondrial stress (Fig. 4, Supplementary Fig. 5). Control cells showed decreases in all respiratory parameters with REN001 treatment while they increased in VLCAD deficient cell lines. VLCAD-1 and VLCAD-3 had the highest increase in basal respiration at 30 nM while VLCAD-2 had the highest increase at 60 nM (Fig. 4A, Supplementary Fig. 4D). The control cell line decreased in basal respiration with an increase in REN001 (Fig. 4A). Similarly, maximal respiration and spare respiratory capacity significantly increased across all VLCAD cell lines and significantly decreased in the control cell line (Figs. 4B, 4C). Calculated ATP production also significantly increased in the VLCADD cell lines with the highest increases at 30 nM or 60 nM (Fig. 4D, Supplementary Fig. 5D).

Previous cellular studies have reported variable results using bezafibrate to improve cellular bioenergetics [30, 38–40]. As a PPAR-d agonist, REN001 should theoretically have more directed action on the targets of interest in VLCADS than bezafibrate. To test this hypothesis, we treated control and VLCADD fibroblasts with 600 µM dezafibrate and measured oxygen consumption rate (Supplementary Fig. 6A). Control cells had decreased basal respiration, maximal respiration and ATP-linked respiration with bezafibrate treatment while there was no statistically significant change in spare respiratory capacity (Fig. 4E-H). VLCAD-1 and − 3 had significantly reduced basal respiration, maximal respiration, and ATP-linked respiration with 600 µM Bezafibrate (Fig. 4E, F, H). VLCAD-4 had no statistically significant differences in basal respiration, maximal respiration, spare respiratory capacity, or ATP-linked respiration (Fig. 4E-H). VLCAD-3 had no statistically significant differences in spare respiratory capacity. VLCAD-2 was an outlier in these experiments, with an improvement in all parameters with bezafibrate treatment (Fig. 4E-H).

ATP Production

An increase in ATP production can be indicative of less cellular stress and increased FAO protein due to REN001 treatment. We therefore directly measured ATP production with a real-time rate ATP assay via a Seahorse XFe96 Extracellular Analyzer. All cell lines significantly increased their total ATP production (Fig. 5C). Glycolytic and mitochondrial ATP production were significantly increased across all VLCADD cell lines (Fig. 5A, 5B).

Acylcarnitine profile analysis

Acylcarnitines in media accumulate from cellular metabolism and a characteristic pattern including increases in long chain saturated and unsaturated species can be detected in media from VLCAD deficient cells, consistent with the profile seen in blood samples from patients. Reduction of these species following REN001 treatment would suggest improved VLCAD function. As expected palmitoylcarnitine (C16) was elevated in growth medium from all of the VLCADD patient fibroblasts, except VLCAD-1, compared to control (Supplementary Fig. 7C). REN001 treatment did not decrease palmitoylcarntine in any VLCADD cell lines treated at the various concentrations (Supplementary Fig. 7C). Palmitoylcarnitine significantly increased at 120 nM treatment in VLCAD-1, -3, and − 4 suggesting that the higher dose of drug is toxic (Supplementary Fig. 7C). No change was seen in the media of VLCAD-2 cells at any drug level. Acetylcarnitine (C2) reflects levels of the acetyl-CoA end product of FAO and is typically lower in VLCAD deficient patients and patient cells. Increased flux through FAO in patient cells could increase acetylcarnitine, though alternative metabolic pathways would utilize increased acetyl-CoA before it can accumulate. An increase in acetylcarnitine was not detected in media of the patient cell lines with REN001 treatments, with VLCAD-1 and − 2 having statistically significant decreased at 30 and 120 nM treatment (Supplementary Fig. 7A). Control cells did not significantly change in acetylcarnitine with REN001 treatment (Supplementary Fig. 7A). Both control and VLCADD cell lines did not statistically increase in C14:1 carnitine media levels, except VLCAD-4 (Supplementary Fig. 7B).

Discussion

There is no effective treatment for VLCAD deficiency. Rather, current treatment protocols rely on dietary restrictions and replenishment of the deficiency in energy using a supplemental dietary energy source such as medium chain triglyceride oil or the newly FDA approved heptanoic acid in the triglyceride form, triheptanoin [11, 12, 41, 42]. However, the treatment is inadequate as episodes of rhabdomyolysis and cardiomyopathy persist. Gene therapy has been reported in mice, but has not been developed further for humans [43].

In this study, we focused on enhancing the expression of genes involved in mitochondrial bioenergetics, including FAO, using the PPARd agonist REN001. We hypothesized that such a treatment could either directly or indirectly improve energy metabolism in cells from patients with VLCAD deficiency partly by raising the amount of partially active mutant VLCAD protein. Our results demonstrated a statistically significant increase in *ACADVL*, *HADHA* and *HADHB* via mRNA analysis following treatment of patient

cells with REN001. Indeed, there was a small increase in protein levels of both VLCAD and TFP protein as well as cellular FAO flux in a dose dependent fashion. More importantly, we demonstrated an improvement in the cellular overall bioenergetic state with REN001 treatment as measured by oxygen consumption and ATP production. These findings, in combination, indicate an improvement in the overall bioenergetic health of patient fibroblasts, and identify REN001's potential as a therapeutic agent for VLCAD deficiency.

Not surprisingly, response of VLCAD deficient cell lines to REN001 was variable given that each had a unique mutant genotype VLCAD protein with variable instability. Similar results have been reported when treating VLCAD deficient fibroblasts with bezafibrate, a pan-PPAR activist with considerably less delta activity that REN001 [30]. In that study, fibroblasts with the most protein damaging mutation had minimal effect with bezafibrate treatment, including no rescue of VLCAD protein. An additional study of VLCADD fibroblast from 33 different patients with 45 different *ACADVL* mutations similarly confirmed that bezafibrate treatment in cells with less damaging point mutations responded better than those with insertions, deletions, or frameshift mutations [39]. A similar finding was evident in our study. Fibroblasts VLCAD-2 (with the most severe predicted mutant genotype/least protein stability) exhibited only a small increase in enzyme activity and protein content with treatment, but no increase in fatty acid oxidation flux, and only minimal improvement in oxygen consumption rate. Of note, VLCADD fibroblasts containing the c.848T > C (p.Val283Ala) (VLCAD-4) and c.520G > A (p.Val174Met) (VLCAD-1) variants behaved similarly with REN001 treatment compared to cell lines containing the same mutations and treated with bezafibrate [39, 40]. Bezafibrate treatment restored FAO flux to 65 to 75% of control, 1.3 to 2.3 fold increase in VLCAD mRNA, and 2.2 to 4.8 fold increase in VLCAD activity in cell lines containing c.848T > C (p.Val283Ala). Bezafibrate treatment also increased FAO flux to 65% of control and 1.3 to 2.3 fold increase in VLCAD mRNA expression in a homozygous c.520G > A (p.Val174Met). In VLCAD-1, 120 nM REN001 treatment did not restore FAO flux, and elicited a minimal increase in VLCAD activity with a 2-fold increase VLCAD mRNA expression. Similarly, REN001 treatment minimally increased FAO flux and VLCAD expression, while VLCAD mRNA expression increased 3.1- fold in VLCAD-4 similar to bezafibrate treatment.

Our results confirm the need for an individual, mutation specific approach for selecting approach drug therapies for VLCADD patients. In considering the use of a PPARd agonist for treatment of patients, it is likely that dosing differences related to the relative delta effects of the drugs are likely to be critical. Thus while, bezafibrate had some activity at high concentrations (400–600 μM) in some previous *in vitro* studies, it was ineffective in others [38], and has not shown efficacy in clinical trials in patients [35]. For the most part, we found worsening or no change in oxygen consumption with bezafibrate treatment, even at 20,000-fold higher concentration bezafibrate (concentration based on previous published studies) compared to REN001. However, one cell line responded to bezafibrate treatment even though the cell line had minimal response with REN001, demonstrating a possible genotype specific effect. Importantly, the minimal effective dose for REN001 in our study was 30 nM, more amendable to dose escalation as needed in patients. A clinical trial for resveratrol, proposed to have both PPARα -γ agonist effects [44],

showed no improvement on fatty acid oxidation or exercise capacity in VLCADD or CPT2 deficient patients [45].

One limitation of this study is that the treatments were performed in patient derived fibroblasts. VLCAD patients suffer from both cardiomyopathy and rhabdomyolysis due to dysfunction of heart and skeletal muscle, respectively [5, 46–49]. Since fibroblasts contain fewer mitochondria compared to both, translation of fibroblast results to patients remains uncertain. Additional experiments in other long chain fatty acid oxidation disorders including TFP, LCHAD, and CPT2 deficiencies are necessary to expand our results to them. An *ACADVL* null mouse model with no residual protein [50, 51] is not ideal for testing REN001 given the lack of VLCAD protein. Rather, a point mutation in *ACADVL* generated via CRISPR/Cas technology would provide additional insight into the drug's effect in a whole organism [52–54].

In summary, our results identify PPARδ agonists, such as REN001, as a potential treatment for VLCAD deficiency, exhibiting a positive effect on enzyme activity and cellular bioenergetics. Since results are mutation specific, a personalized medicine approach will be necessary to assess the likelihood of utility based on their mutation status.

Materials And Methods

Experiments were performed in accordance with approved local and regional guidelines and regulations. Experimental human protocols were approved by the Institutional Review Board at the University of Pittsburgh, protocol 19030195.

Subjects

Skin biopsies for fibroblast culture were performed on a clinical basis from patients with various mutations in *ACADVL* with written informed consent from patients and/or parents (Table 1). Control fibroblast cells were obtained from American Type Culture Collection (ATCC.org).

Table 1: List of VLCAD deficient cell lines used in this project with their corresponding mutations in *ACADVL* and phenotypic severity.

Cell Line	Laboratory Designation	Mutations	Phenotypic Severity
Control-1	FB826	N/A	Control
Control-2	FB549	N/A	Control
Control-3	FB902	N/A	Control
VLCAD-1	FB833	c.520G>A (p.Val174Met)/c.1825G>A (p.Glu609Lys)	Mild
VLCAD-2	FB671	c.1619T>C (p.Leu540Pro)/c.1707-1715dup (p.Asp570_Ala572dup)	Severe
VLCAD-3	FB863	c.896_898del (p.Lys299del)/c.1147C>G (p.Leu383Val)	Mild
VLCAD-4	FB782	c.848T>C (p.Val283Ala)/c.1258A>C (p.Ile420Leu)	Mild

Cell culture and treatments

Cell lines were grown in Dulbecco's Modified Eagle Medium (DMEM, Corning Life Sciences, Manassas, VA), containing high glucose levels (4.5 g/L) or in DMEM devoid of glucose for 48 hr. Both media were supplemented with 10% fetal bovine serum (FBS), 4 mM L-glutamine, and 100 IU penicillin and 100 µg/ml streptomycin (Corning Life Sciences). REN001 was obtained from Reneo Pharmaceuticals, Irvine, CA, and resuspended from a powder in DMSO.

Cells were treated with REN001 at 85% confluency at the following concentrations: 0, 15, 30, 60 and 120 nM. Additional cultures were treated with 600 µM bezafibrate (Sigma Aldrich, St. Louis, MO). The 0 nM treatment was given DMSO as a control for both REN001 and Bezafibrate. Cultures were incubated for 48 hr at 37°C, 5% CO_2 and were harvested for analysis.

Real-time quantitative polymerase chain reaction (qPCR)

Total RNA was isolated using the RNeasy Mini Kit (Qiagen, Valencia, CA) from REN001 treated VLCAD and control fibroblast with on column DNaseI digestion (Qiagen). First strand synthesis of complementary DNA (cDNA) was reverse-transcribed from 2,500 ng of total RNA using the Super Vilo IV Master Mix (Qiagen). Quantitative PCR was performed with equivalent amount of cDNA on a Bio-Rad CFX96 Real-Time PCR Instrument, with SYBR Green Master Mix (Thermo Fisher Scientific, Waltham, MA). *ACADVL*, *HADHA*, *HADHB*, *ETFDH*, *UQCRC2* and *NDUFS2* were assayed using primers were obtained from PrimerBank [55–57] (Supplementary Table 1). Expression levels were normalized to *TOMM20* and the data were analyzed by the $2^{-\Delta\Delta Ct}$ method [58].

PPARδ binding site analysis

ChIP-seq analysis for PPARδ binding sites was performed using the publicly available dataset on Gene Expression Omnibus (GSE 50144) (PMID: 24721177), and binding sites were identified with the use of MACS2 (PMID: 24743991). ChIP-seq peaks were visualized using the IGV viewer (PMID: 21221095), and gene ontology enrichment for PPARδ target genes and pathways were analyzed using the Cistrome-GO and GREAT GO tools (PMID: 20436461) (PMID: 31053864).

Whole cell lysate, protein concentration, SDS-PAGE gel, and western blot

Cell were treated with REN001 in complete DMEM with glucose for 48 hr, harvested via trypsinization, pelleted, and stored at -80°C for western blot analysis. Pellets were lysed with 50 µl of radioimmunoprecipitation assay (RIPA) buffer (Thermo Fisher Scientific) with 1X Protease Inhibitor Cocktail (PI) (Roche, St. Louis, MO) for 30 min on ice and centrifuged at 14,000 x g for 15 min at 4°C. Supernatants were collected and 25 µg of protein was loaded onto a 4–15% gradient Criterion precast SDS-PAGE gel (Bio-Rad, Hercules, CA). Following electrophoresis, the gel was blotted onto a nitrocellulose membrane and incubated with anti-VLCAD (VLCAD 1:1000, rabbit, Vockley lab), then incubated with secondary goat anti-rabbit-HRP antibody (1:3000, BioRad). Pierce ECL Western Blotting Substrate kit (Thermo Fisher Scientific) was used to visualize bands. Membranes were stripped and re-probed with TFP cocktail antibody (1:1000, rabbit, Vockley lab, [59]) containing antibodies for both the alpha and beta subunits, and with mouse-anti-glyceraldehyde 3-phosphate dehydrogenase (GAPDH; 1:25000) monoclonal antibody (ABCAM, Cambridge, MA) to verify equal loading. ImageLab software was used to quantify band intensity and bands were normalized to GAPDH intensity.

Immunofluorescence microscopy

Treated cultured fibroblasts were seeded at a concentration of $5x10^4$ cells/mL on Poly-L-Lysine coated glass cover slips in a 12-well plate and allowed to grow overnight in growth media at 37°C in a 5% CO_2 incubator. Cells were then fixed in 4% paraformaldehyde for 10 min and permeabilized with 0.1% Triton X100 and blocked after brief washings in 5% donkey serum at room temperature for 1 hr. Cells were briefly washed and treated with primary antibodies VLCAD (1:1000, Vockley Lab) and HADHA (1:100, Santa Cruz Biotechnology, Dallas, TX) overnight in 4°C. After brief washing with 1 X TBST, cells were incubated with the secondary antibodies donkey anti-rabbit Alexa Fluor 488 and donkey anti-mouse Alexa Fluor 594 (1:1000, Invitrogen, Waltham, MA) for 1 hr at RT. Nuclei were immunostained with NucBlue Fixed Cell ReadyProbes Reagent (DAPI; Invitrogen). The cover slips were then mounted using mounting media before imaging. All images were taken on a Zeiss LSM Confocal microscope using 63X magnification. Images were analyzed using ImageJ [60].

Electron transfer flavoprotein (ETF) fluorometric reduction assay

The ETF reduction assay was performed using a Jasco FP-6300 spectrofluorometer (Easton, MD) with a cuvette holder heated with circulating water at 32°C as previously described [61]. Briefly, treated cell

pellets were lysed using 50 mM Tris, pH 8.0 buffer and 0.1 X protease inhibitor EDTA-free and sonicated twice in an ice cold water bath sonicator at amplitude 45 for 1.5 min with 15 sec intervals. The assay was otherwise performed as described, at the indicated substrate concentrations [61]. The enzyme was diluted 1200-fold into buffer containing 50 mM Tris, pH 8.0, 5 mM EDTA and 50% glycerol, and 10 µl was used for each assay. The ETF concentration was 2 µM. Spectra Manager 2 software (Jasco, Inc.) was used to collect data and calculate reaction rate and Microsoft Excel was used to calculate the kinetic parameters.

Fatty acid oxidation (FAO) flux analysis

Tritium-release assay was performed as previously described with the noted changes [62]. Cells were grown in T175 flasks and seeded at 350,000 cells per well in 6-well plates in triplicates and in duplicate wells for protein concentration for normalization, and grown for 24 hr in complete DMEM. Wells were treated with REN001 in complete DMEM for 48 hr in 37°C/5% CO_2 incubator. Cells were washed once with PBS and incubated with 0.34 µCi [9,10-^{3}H] oleate (45.5Ci/mmol; Perkin Elmer, Waltham, MA) in 50 nmol of oleate prepared in 0.5 ml glucose-free DMEM with 1 µg/ml L-carnitine and 2 mg/ml alpha-cyclodextrin for 2 hr at 37°C. Fatty acids were solubilized with alpha-cyclodextrin as described [63]. After incubation ^3H_2O released was separated from the oleate on a column containing 750 µl of anion exchange resin (AG 1 x 8, acetate, 100–200 Mesh, BioRad) prepared in water. After the incubation medium was passed through the column, the plate was washed with 1 ml of water, which was also transferred to the column, and resin was washed with 1 ml of water. All eluates were collected in a scintillation vial and mixed with 10 ml of scintillation fluid (Eco-lite, MP), followed by counting in a Beckman scintillation counter in the tritium window. Standards contained a 10 µl aliquot of the incubation mix with 3 ml of deionized water and 10 ml of scintillation fluid.

Measurement of mitochondrial respiration

Oxygen consumption rate (OCR) was measured with a Seahorse XF^{e}96 Extracellular Flux Analyzer Cell Mito Stress Test Kit (Agilent Technologies, Santa Clara, CA). Fibroblasts were treated with REN001or bezafibrate resuspended in DMSO in DMEM without glucose for 48 hr in 37°C/5% CO_2 incubator. Fibroblasts were harvested and seeded at a density of 60,000 cells per well in a 96-well seahorse plate coated in poly-D-lysine the day of assay. Plate was centrifuged at 300 rpm for 1 min, rotated, and centrifuged again at the same settings. Cells were incubated in for 1 hr without CO_2 in buffered Seahorse XF Assay Media (Agilent Technologies) and supplemented with 1 mM sodium pyruvate and 2 mM L-glutamine. Manufacturer's directions were otherwise followed for the XF Mito Stress Test kit (Agilent Technologies).

Measurement of ATP production

Glycolytic and mitochondrial ATP production was measured with a Seahorse XF^{e}96 Extracellular Flux Analyzer with a XF Real-Time ATP Rate Assay kit (Agilent Technologies). Fibroblasts were seeded at 40,000 cells per well in complete DMEM and grown overnight at 37°C/5% CO_2 incubator. Growth media was removed and fibroblasts were treated with REN001 in complete DMEM for 48 hrs. Cells were washed

twice with water and incubated in for 1 hr without CO_2 in buffered Seahorse XF Assay Media (Agilent Technologies) supplemented with 1 mM sodium pyruvate, 2 mM L-glutamine, and 10 mM L-glucose. Manufacturer's directions were otherwise followed for the Real-Time ATP Rate assay kit (Agilent Technologies).

Acylcarnitine profile analysis

Acylcarnitine profiles were determined as previously described [64–66]. Cells were seeded at 350,000 cells per well in 6-well plates in triplicates in complete DMEM. Growth media was changed to Ham's F12 media (Gibco, Waltham, MA) supplemented with 10% FBS, 4 mM L-glutamine, and 100 IU penicillin and 100 µg/ml streptomycin (Corning Life Sciences) for 24 hr. Wells were incubated with REN001 200 µM palmitic acid, 400 µM L-carnitine, and 0.4% fatty acid free BSA in Minimum Essential Medium (MEM; Gibco) with no supplementation. Plates were incubated in a 37°C/5% CO_2 incubator for 72 hr. Media was collected, cells were lysed with 250 µL of RIPA buffer for 30 min at room temperature, and protein concentration was determined.

Aliquots (75 µL) of medium were mixed with methanol (20 µL) containing isotopelabeled carnitine standards and the protein precipitated by addition of absolute ethanol (905 µL) and centrifugation (13,000 rpm, 10 min). A portion of the supernatant (50 µL) was dried under a stream of nitrogen gas and the acylcarnitine butyl esters generated by reaction (60°C for 15 min) in 100 µL of 3N HCl in butanol. Dried residues were reconstituted in acetonitrile-water (80:20) for flow injection ESI-MS-MS analysis. Analysis was performed on a triple quadrupole API4000 mass spectrometer (AB Sciex™, Framingham, MA) equipped with a ExionLC™ 100 HPLC system (Shimadzu Scientific Instruments™, Columbia, MD). Analyst™ (V1.6.3, AB Sciex ©2015) was utilized for data acquisition and ChemoView™ software (V2.0.3, AB Sciex ©2014) for quantitation using isotopelabeled carnitine standards. Acylcarnitine standards were purchased from Amsterdam UMC – VUmc (Amsterdam, NL) and Cambridge Isotope Laboratories, Inc. (Andover, MA). Acylcarnitines were measured using multiple reaction monitoring (MRM) for free carnitine (C0, m/z 218 > m/z 103) and acetylcarnitine (C2, m/z 260 > m/z 85) and Precursor Scan for precursor ions (Q1) of acylcarnitines (C3 to C18, scan range m/z 270 to 502) that generated a product ion (Q3) at *m/z* 85.

Statistical analysis

Calculations were performed in Microsoft Excel. Student's *t* test was used to determine statistical significance in Prism GraphPad (Version 7, graphpad.com).

DATA AVAILABILITY STATEMENT

All datasets generated during and/or analyzed during the current study are available upon request as mandated by NIH guidelines.

Declarations

ACKNOWLEDGEMENTS

J.V. was supported in part by NIH grant R01 DK109907 and from a research grant from Reneo Pharmaceuticals. We thank Yuxun Zhang, PhD from Eric Goetzman, PhD Laboratory, University of Pittsburgh, Children's Hospital of UPMC for ETF supply for the ETF fluorescence reduction assays.

Author Contribution Statement

O.M.D. reviewed literature, performed the majority of experiments, and drafted manuscript. O.M.D., A.W.M., and J.V. developed the experimental design. Y.L.P., developed and performed ChIPseq analysis. A.K. assisted with laboratory studies. C.V.L. performed acylcarnitine analysis on tandem mass spectrometry. A.D. reviewed the manuscript. A.W.M. and J.V. oversaw the work and reviewed the manuscript. All authors reviewed the manuscript.

Competing Interests Statement

J.V. has received research funding from Reneo Pharmaceuticals, Inc. for this project, as well as for participating in clinical trials. A.R. is employed by Reneo Pharmaceuticals, Inc. O.M.D., Y.L.P., A.K., C.V.L., and A.W.M. have no competing interests.

References

1. Fillmore, N., Alrob, O. A., Lopaschuk, G. D., *Fatty Acid beta-Oxidation*. 2014, American Oil Chemistry Society: AOCS Lipid Library.
2. Houten, S.M. and R.J. Wanders, *A general introduction to the biochemistry of mitochondrial fatty acid beta-oxidation*. J Inherit Metab Dis, 2010. **33**(5): p. 469–77.
3. Talley, J.T. and S.S. Mohiuddin, *Biochemstry, Fatty Acid Oxidation*, in *StatPearls*. 2020: Treasure Island (FL).
4. Wang, Y., et al., *Mitochondrial fatty acid oxidation and the electron transport chain comprise a multifunctional mitochondrial protein complex*. J Biol Chem, 2019. **294**(33): p. 12380–12391.
5. Leslie, N.D., et al., *Very Long-Chain Acyl-Coenzyme A Dehydrogenase Deficiency*, in *GeneReviews((R))*, M.P. Adam, et al., Editors. 1993: Seattle (WA).
6. McHugh, D., et al., *Clinical validation of cutoff target ranges in newborn screening of metabolic disorders by tandem mass spectrometry: a worldwide collaborative project*. Genet Med, 2011. **13**(3): p. 230–54.
7. American College of Medical Genetics Newborn Screening Expert, G., *Newborn screening: toward a uniform screening panel and system–executive summary*. Pediatrics, 2006. **117**(5 Pt 2): p. S296-307.
8. Andersen, R.M., *Revisiting the behavioral model and access to medical care: does it matter?* J Health Soc Behav, 1995. **36**(1): p. 1–10.

9. Solis, J.O. and R.H. Singh, *Management of fatty acid oxidation disorders: a survey of current treatment strategies*. J Am Diet Assoc, 2002. **102**(12): p. 1800–3.
10. Behrend, A.M., et al., *Substrate oxidation and cardiac performance during exercise in disorders of long chain fatty acid oxidation*. Mol Genet Metab, 2012. **105**(1): p. 110–5.
11. Gillingham, M.B., et al., *Triheptanoin versus trioctanoin for long-chain fatty acid oxidation disorders: a double blinded, randomized controlled trial*. J Inherit Metab Dis, 2017. **40**(6): p. 831–843.
12. Vockley, J., et al., *Triheptanoin treatment in patients with pediatric cardiomyopathy associated with long chain-fatty acid oxidation disorders*. Mol Genet Metab, 2016. **119**(3): p. 223–231.
13. Vockley, J., *Long-chain fatty acid oxidation disorders and current management strategies*. Am J Manag Care, 2020. **26**(7 Suppl): p. S147-S154.
14. Marsden, D., C.L. Bedrosian, and J. Vockley, *Impact of newborn screening on the reported incidence and clinical outcomes associated with medium- and long-chain fatty acid oxidation disorders*. Genet Med, 2021. **23**(5): p. 816–829.
15. Evans, R.M., G.D. Barish, and Y.X. Wang, *PPARs and the complex journey to obesity*. Nat Med, 2004. **10**(4): p. 355–61.
16. Michalik, L., et al., *International Union of Pharmacology. LXI. Peroxisome proliferator-activated receptors*. Pharmacol Rev, 2006. **58**(4): p. 726–41.
17. Poulsen, L., M. Siersbaek, and S. Mandrup, *PPARs: fatty acid sensors controlling metabolism*. Semin Cell Dev Biol, 2012. **23**(6): p. 631–9.
18. Burdick, A.D., et al., *The role of peroxisome proliferator-activated receptor-beta/delta in epithelial cell growth and differentiation*. Cell Signal, 2006. **18**(1): p. 9–20.
19. Wang, Y.X., et al., *Peroxisome-proliferator-activated receptor delta activates fat metabolism to prevent obesity*. Cell, 2003. **113**(2): p. 159–70.
20. Tanaka, T., et al., *Activation of peroxisome proliferator-activated receptor delta induces fatty acid beta-oxidation in skeletal muscle and attenuates metabolic syndrome*. Proc Natl Acad Sci U S A, 2003. **100**(26): p. 15924–9.
21. Fredenrich, A. and P.A. Grimaldi, *PPAR delta: an uncompletely known nuclear receptor*. Diabetes Metab, 2005. **31**(1): p. 23–7.
22. Forman, B.M., J. Chen, and R.M. Evans, *Hypolipidemic drugs, polyunsaturated fatty acids, and eicosanoids are ligands for peroxisome proliferator-activated receptors alpha and delta*. Proc Natl Acad Sci U S A, 1997. **94**(9): p. 4312–7.
23. Schmidt, A., et al., *Identification of a new member of the steroid hormone receptor superfamily that is activated by a peroxisome proliferator and fatty acids*. Mol Endocrinol, 1992. **6**(10): p. 1634–41.
24. Riserus, U., et al., *Activation of peroxisome proliferator-activated receptor (PPAR)delta promotes reversal of multiple metabolic abnormalities, reduces oxidative stress, and increases fatty acid oxidation in moderately obese men*. Diabetes, 2008. **57**(2): p. 332–9.

25. Oliver, W.R., Jr., et al., *A selective peroxisome proliferator-activated receptor delta agonist promotes reverse cholesterol transport*. Proc Natl Acad Sci U S A, 2001. **98**(9): p. 5306–11.
26. Feng, L., et al., *Bavachinin, as a novel natural pan-PPAR agonist, exhibits unique synergistic effects with synthetic PPAR-gamma and PPAR-alpha agonists on carbohydrate and lipid metabolism in db/db and diet-induced obese mice*. Diabetologia, 2016. **59**(6): p. 1276–86.
27. Misawa, K., et al., *Ginger extract prevents high-fat diet-induced obesity in mice via activation of the peroxisome proliferator-activated receptor delta pathway*. J Nutr Biochem, 2015. **26**(10): p. 1058–67.
28. Fedorova, L.V., et al., *Peroxisome proliferator-activated receptor delta agonist, HPP593, prevents renal necrosis under chronic ischemia*. PLoS One, 2013. **8**(5): p. e64436.
29. Information, N.C.f.B., *Bezafibrate, CID = 39042*. 2019: PubChem Database.
30. Djouadi, F., et al., *Bezafibrate increases very-long-chain acyl-CoA dehydrogenase protein and mRNA expression in deficient fibroblasts and is a potential therapy for fatty acid oxidation disorders*. Hum Mol Genet, 2005. **14**(18): p. 2695–703.
31. Djouadi, F., et al., *Peroxisome proliferator activated receptor delta (PPARdelta) agonist but not PPARalpha corrects carnitine palmitoyl transferase 2 deficiency in human muscle cells*. J Clin Endocrinol Metab, 2005. **90**(3): p. 1791–7.
32. Djouadi, F., et al., *Mitochondrial trifunctional protein deficiency in human cultured fibroblasts: effects of bezafibrate*. J Inherit Metab Dis, 2016. **39**(1): p. 47–58.
33. Yamada, K., et al., *Open-label clinical trial of bezafibrate treatment in patients with fatty acid oxidation disorders in Japan*. Mol Genet Metab Rep, 2018. **15**: p. 55–63.
34. Shiraishi, H., et al., *Open-label clinical trial of bezafibrate treatment in patients with fatty acid oxidation disorders in Japan; 2nd report QOL survey*. Mol Genet Metab Rep, 2019. **20**: p. 100496.
35. Orngreen, M.C., et al., *Bezafibrate in skeletal muscle fatty acid oxidation disorders: a randomized clinical trial*. Neurology, 2014.
36. Fang, L., et al., *PPARgene: A Database of Experimentally Verified and Computationally Predicted PPAR Target Genes.* PPAR Res, 2016. **2016**: p. 6042162.
37. Diekman, E.F., et al., *Fatty acid oxidation flux predicts the clinical severity of VLCAD deficiency*. Genet Med, 2015. **17**(12): p. 989–94.
38. Seminotti, B., et al., *Mitochondrial energetics is impaired in very long-chain acyl-CoA dehydrogenase deficiency and can be rescued by treatment with mitochondria-targeted electron scavengers*. Hum Mol Genet, 2019. **28**(6): p. 928–941.
39. Gobin-Limballe, S., et al., *Genetic basis for correction of very-long-chain acyl-coenzyme A dehydrogenase deficiency by bezafibrate in patient fibroblasts: toward a genotype-based therapy*. Am J Hum Genet, 2007. **81**(6): p. 1133–43.
40. Gobin-Limballe, S., et al., *Compared effects of missense mutations in Very-Long-Chain Acyl-CoA Dehydrogenase deficiency: Combined analysis by structural, functional and pharmacological approaches*. Biochim Biophys Acta, 2010. **1802**(5): p. 478–84.

41. Gillingham, M.B., et al., *Metabolic control during exercise with and without medium-chain triglycerides (MCT) in children with long-chain 3-hydroxy acyl-CoA dehydrogenase (LCHAD) or trifunctional protein (TFP) deficiency*. Mol Genet Metab, 2006. **89**(1–2): p. 58–63.
42. Pervaiz, M.A., et al., *MCT oil-based diet reverses hypertrophic cardiomyopathy in a patient with very long chain acyl-coA dehydrogenase deficiency*. Indian J Hum Genet, 2011. **17**(1): p. 29–32.
43. Keeler, A.M., et al., *Long-term correction of very long-chain acyl-coA dehydrogenase deficiency in mice using AAV9 gene therapy*. Mol Ther, 2012. **20**(6): p. 1131–8.
44. Calleri, E., et al., *Resveratrol and its metabolites bind to PPARs*. Chembiochem, 2014. **15**(8): p. 1154–1160.
45. Storgaard, J.H., et al., *No effect of resveratrol on fatty acid oxidation or exercise capacity in patients with fatty acid oxidation disorders: a randomized clinical cross-over trial*. J Inherit Metab Dis, 2022.
46. Aoyama, T., et al., *A novel disease with deficiency of mitochondrial very-long-chain acyl-CoA dehydrogenase*. Biochem Biophys Res Commun, 1993. **191**(3): p. 1369–72.
47. Wood, J.C., et al., *Diagnosis of very long chain acyl-dehydrogenase deficiency from an infant's newborn screening card*. Pediatrics, 2001. **108**(1): p. E19.
48. Miller, M.J., et al., *Recurrent ACADVL molecular findings in individuals with a positive newborn screen for very long chain acyl-coA dehydrogenase (VLCAD) deficiency in the United States*. Mol Genet Metab, 2015. **116**(3): p. 139–45.
49. Wanders, R.J., et al., *Disorders of mitochondrial fatty acyl-CoA beta-oxidation*. J Inherit Metab Dis, 1999. **22**(4): p. 442–87.
50. Cox, K.B., et al., *Gestational, pathologic and biochemical differences between very long-chain acyl-CoA dehydrogenase deficiency and long-chain acyl-CoA dehydrogenase deficiency in the mouse*. Hum Mol Genet, 2001. **10**(19): p. 2069–77.
51. Cox, K.B., et al., *Cardiac hypertrophy in mice with long-chain acyl-CoA dehydrogenase or very long-chain acyl-CoA dehydrogenase deficiency*. Lab Invest, 2009. **89**(12): p. 1348–54.
52. Ran, F.A., et al., *Genome engineering using the CRISPR-Cas9 system*. Nat Protoc, 2013. **8**(11): p. 2281–2308.
53. Kraft, K., et al., *Deletions, Inversions, Duplications: Engineering of Structural Variants using CRISPR/Cas in Mice*. Cell Rep, 2015. **10**(5): p. 833–839.
54. Yoshimi, K., et al., *ssODN-mediated knock-in with CRISPR-Cas for large genomic regions in zygotes*. Nat Commun, 2016. **7**: p. 10431.
55. Wang, X. and B. Seed, *A PCR primer bank for quantitative gene expression analysis*. Nucleic Acids Res, 2003. **31**(24): p. e154.
56. Spandidos, A., et al., *A comprehensive collection of experimentally validated primers for Polymerase Chain Reaction quantitation of murine transcript abundance*. BMC Genomics, 2008. **9**: p. 633.
57. Wang, X., et al., *PrimerBank: a PCR primer database for quantitative gene expression analysis, 2012 update*. Nucleic Acids Res, 2012. **40**(Database issue): p. D1144-9.

58. Livak, K.J. and T.D. Schmittgen, *Analysis of relative gene expression data using real-time quantitative PCR and the 2(-Delta Delta C(T)) Method*. Methods, 2001. **25**(4): p. 402–8.
59. Schiff, M., et al., *Molecular and cellular pathology of very-long-chain acyl-CoA dehydrogenase deficiency*. Mol Genet Metab, 2013. **109**(1): p. 21–7.
60. Schneider, C.A., W.S. Rasband, and K.W. Eliceiri, *NIH Image to ImageJ: 25 years of image analysis*. Nat Methods, 2012. **9**(7): p. 671–5.
61. Frerman, F.E. and S.I. Goodman, *Fluorometric assay of acyl-CoA dehydrogenases in normal and mutant human fibroblasts*. Biochem Med, 1985. **33**(1): p. 38–44.
62. Leipnitz, G., et al., *Evaluation of mitochondrial bioenergetics, dynamics, endoplasmic reticulum-mitochondria crosstalk, and reactive oxygen species in fibroblasts from patients with complex I deficiency*. Sci Rep, 2018. **8**(1): p. 1165.
63. Watkins, P.A., et al., *Peroxisomal fatty acid beta-oxidation in HepG2 cells*. Arch Biochem Biophys, 1991. **289**(2): p. 329–36.
64. Okun, J.G., et al., *A method for quantitative acylcarnitine profiling in human skin fibroblasts using unlabelled palmitic acid: diagnosis of fatty acid oxidation disorders and differentiation between biochemical phenotypes of MCAD deficiency*. Biochim Biophys Acta, 2002. **1584**(2–3): p. 91–8.
65. Shen, J.J., et al., *Acylcarnitines in fibroblasts of patients with long-chain 3-hydroxyacyl-CoA dehydrogenase deficiency and other fatty acid oxidation disorders*. J Inherit Metab Dis, 2000. **23**(1): p. 27–44.
66. Smith, E.H. and D. Matern, *Acylcarnitine analysis by tandem mass spectrometry.* Curr Protoc Hum Genet, 2010. Chapter 1**7**: p. Unit 17 8 1–20.

Figures

Figure 1

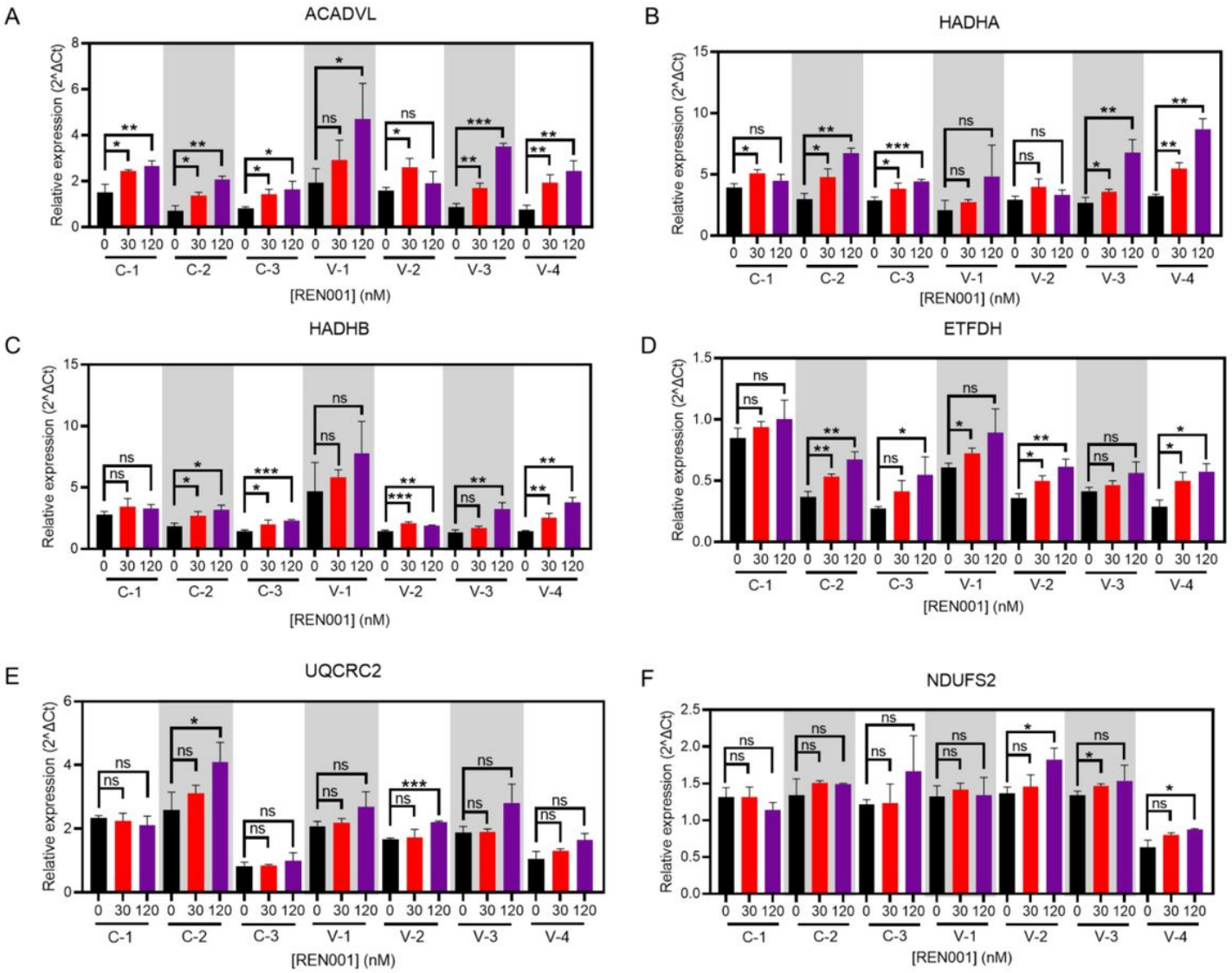

Figure 1

qPCR in control (C-1, 2, 3) and VLCAD deficient (V-1, 2, 3) fibroblasts treated with REN001 at 30 or 120 nM final concentration for 48 hr. Bars represent mean and standard deviations. *p < 0.05, **p < 0.01, ***p < 0.001, ns = not significant, compared to itself at 0 nM treatment (n = 3 for all assays; t test for unpaired samples).

Figure 2

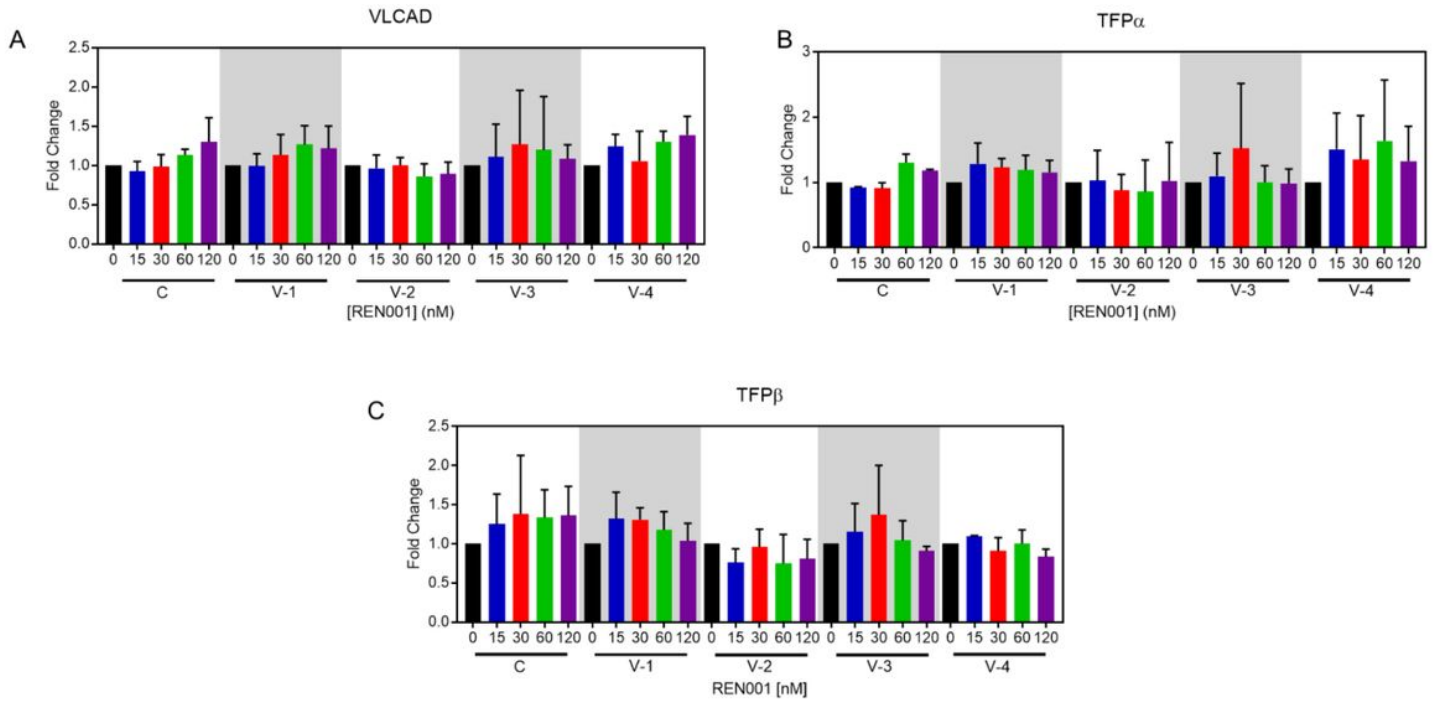

Figure 2

VLCAD (A), TFPα (B), and TFPβ (C) cellular protein content was quantified from western blots of whole cell lysates prepared from REN001 treated fibroblasts. Data are presented as fold changes compared to itself at 0 nM treatment (n = 3 for all assays).

Figure 3

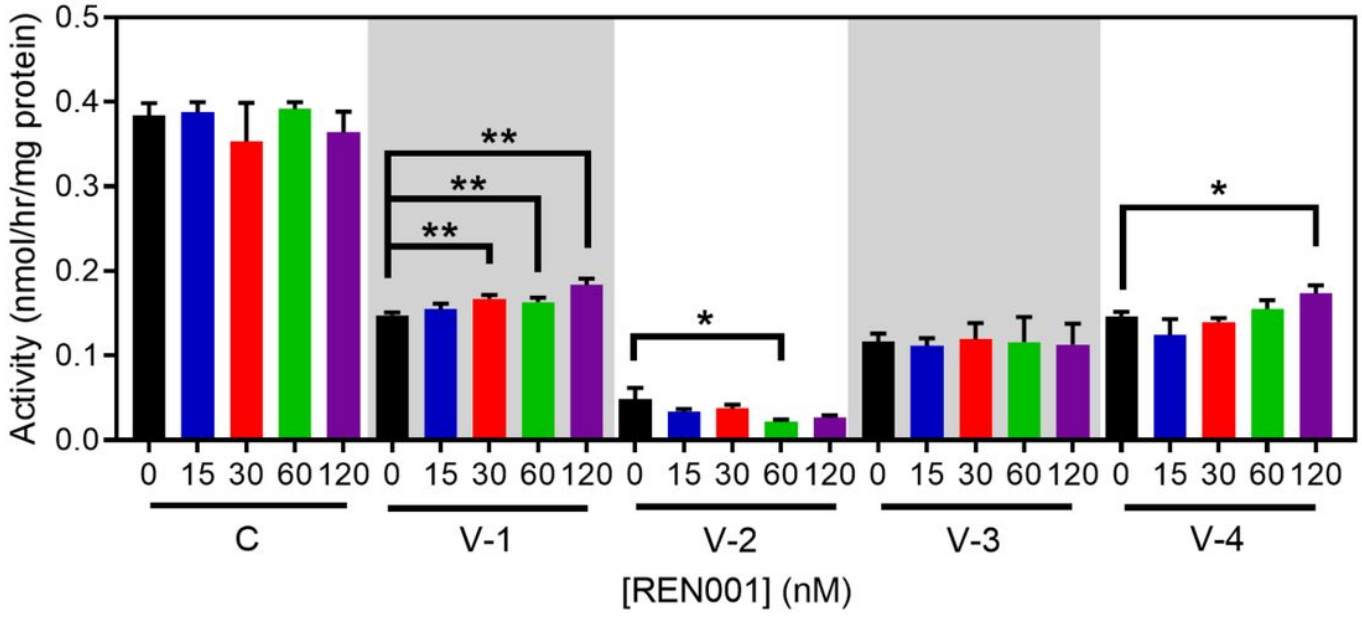

Figure 3

Fatty acid oxidation (FAO) flux in control and VLCAD deficient fibroblasts treated with REN001 for 48 hr. Bars represent mean and standard deviations in duplicate assays. *p < 0.05, **p < 0.01, compared to itself at 0 nM treatment (n = 3 for all assays; *t* test for unpaired samples).

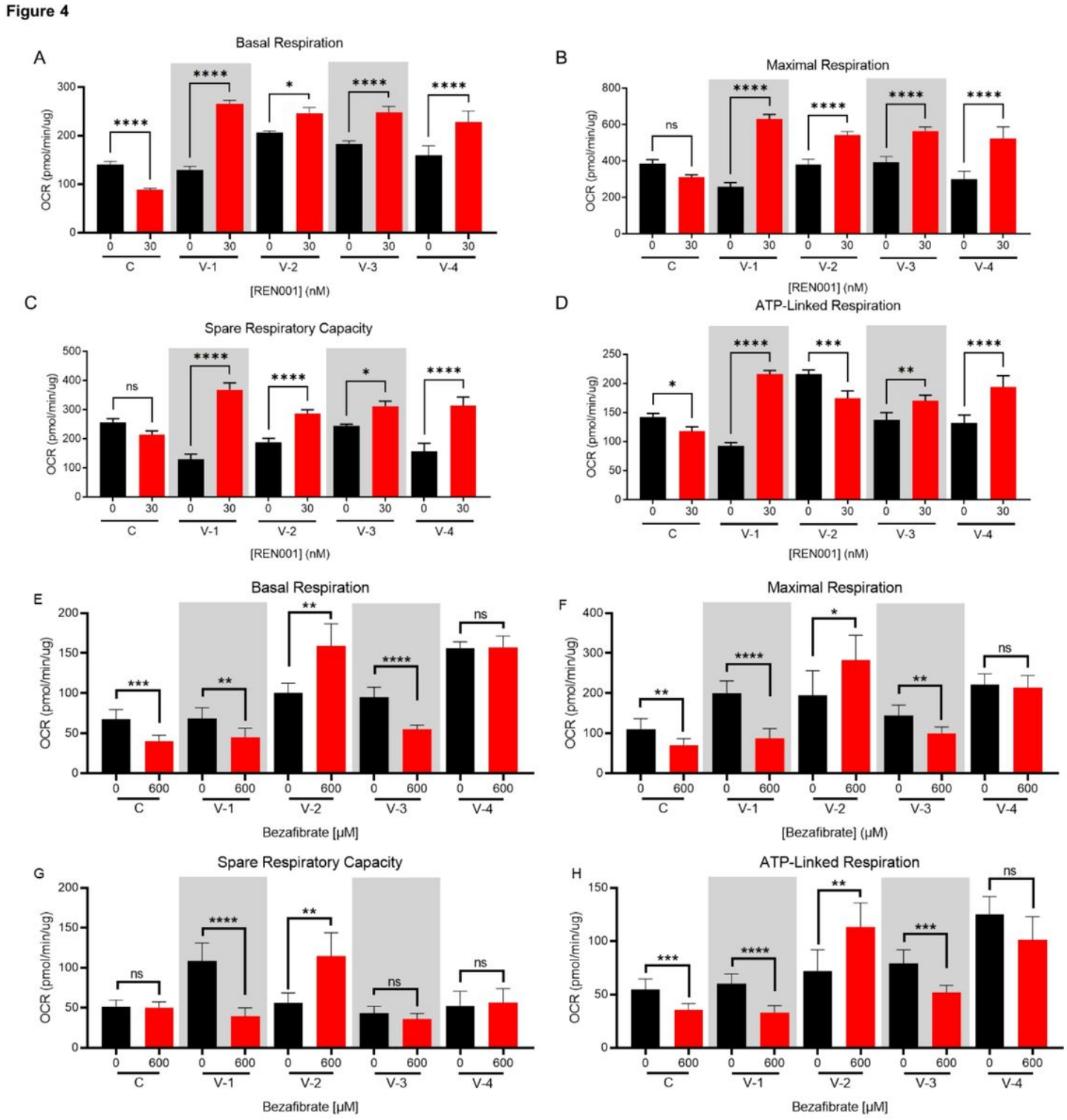

Figure 4

Oxygen consumption rate of control and VLCAD deficient cell lines treated with REN001 for 48 hr. Basal respiration (A), maximal respiration (B), spare respiratory capacity (C), and ATP production (D). Bars represent mean and standard deviations in duplicate assays. *p < 0.05, **p < 0.01, ***p <0.001, ****p < 0.0001, ns = no significant, compared to each cell lines own 0 nM treatment (n = 6 for all assays; *t* test for unpaired samples).

Figure 5

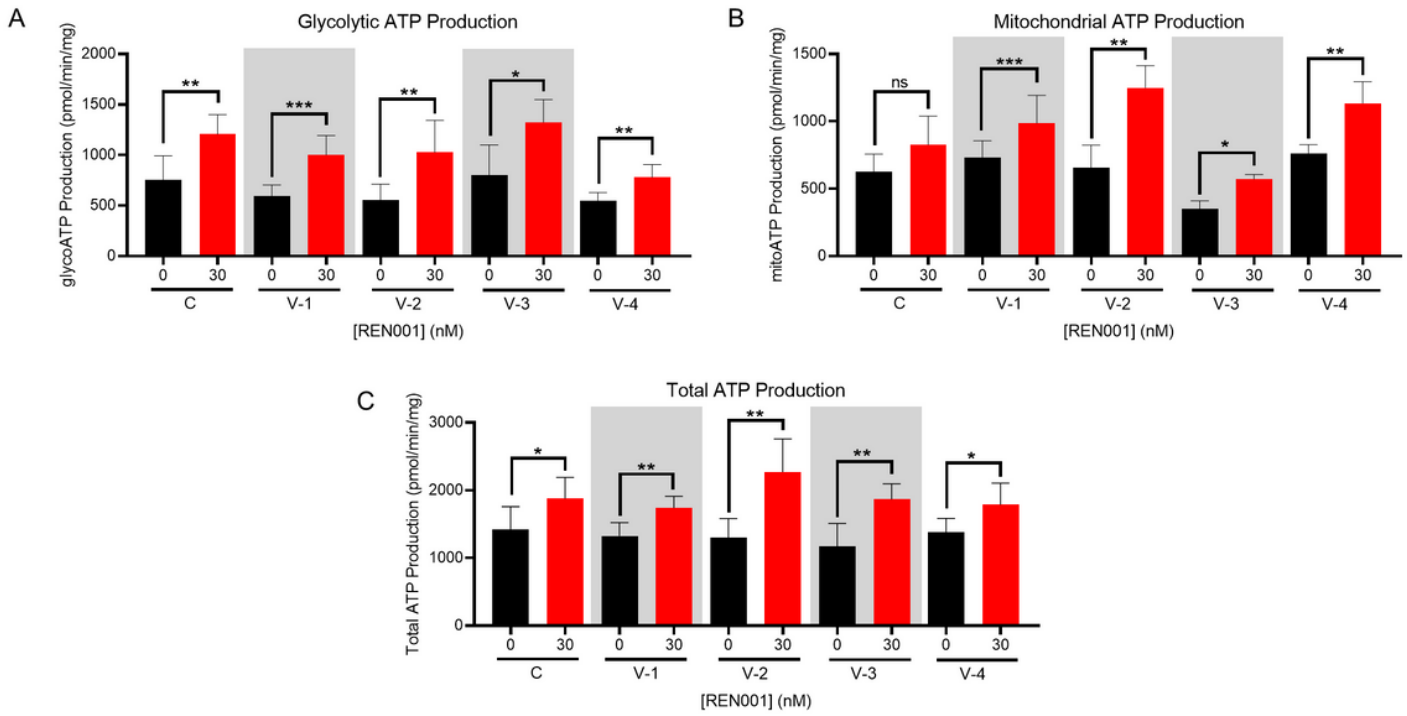

Figure 5

Real-time ATP production measured in control and VLCAD deficient fibroblasts treated with REN001 for 48 hr. Bars represent mean and standard deviations. *p < 0.05, **p < 0.01, p<0.001, ns = not significant, compared to itself at 0 nM treatment (n = 6 for all assays; *t* test for unpaired samples).

Supplementary Files

This is a list of supplementary files associated with this preprint. Click to download.

- DAnnibaleVLCADDPPARAgonistTreatmentManuscriptSupplemental2022.docx